



Research article

Flexural, compression and fracture properties of epoxy granite as a cost-effective structure materials: new machine element foundation

Mohammed Y. Abdellah^{1,2,*}, Ahmed Abdelhaleem¹, Ibrahim A. Alnaser^{2,3}, G. T. Abdel-Jaber¹ and Abdalla Abdal-hay^{1,4}

¹ Mechanical Engineering Department, Faculty of Engineering, South Valley University, Qena, 83523, Egypt

² Mechanical Engineering Department, College of Engineering and Islamic Architecture, Umm Al-Qura University Makkah, KSA

³ Department of Mechanical and Industrial Engineering, College of Engineering, Majmaah University, Al-Majmaah 11952, Saudi Arabia

⁴ School of Dentistry, The University of Queensland, Herston Campus, 4072, Australia

* **Correspondence:** Email: mohamed_abdalla@eng.svu.edu.eg, mohammed_yahya42@yahoo.com.

Abstract: Epoxy granite (EG) as a composite material has been attempted to be used in machine foundation. EG demonstrates similar mechanical properties and specific density to light metals, such as aluminium and its alloys. In the present study, we developed light and cost-effective EG composite materials as a new machine element foundation. The EG composite was prepared by blending the epoxy resin (12 wt%) and granite particles by casting route method. The crushed granite particles were sieved and separated into coarse particles 1.18–2.36 mm, medium particles 0.6–1.18 mm and fine particles ≤ 0.6 mm. The mechanical properties such as compression, bending and single edge notch bending tests were assessed. The results show that the EG composite materials containing the fine granite particles induced the highest compressive (18.1 MPa) and bending (20.1 MPa) strength. In addition, the fracture toughness had the highest value which was about $24.73 \text{ MPa}\sqrt{\text{m}}$ of the same EG composite material. Our results suggest that the EG composite contains fine granite particles with good mechanical and fracture properties might have a high potential in machine foundation application as an inexpensive material.

Keywords: epoxy granite; fracture toughness; composite

1. Introduction

Although the cast iron is widely utilized in machine element foundation because it possesses good impact/fracture and thermal properties, it lacks machining capability. The final product of the cast iron based materials such as the roughness and net-shapes needs high accuracy machining tools. In addition, at high operating speed the conventional cast iron and steel structure materials develop positional error due to the low dynamic stability of these materials. Therefore, it is mandatory to find alternative cost-effective materials that can be used as a machine element foundation. Recent attempts have been paid to use epoxy resin as a matrix contains macro-micro scale particles as a filler material to enhance the mechanical properties and thermal stability. Researchers [1,2] studied the use of cementitious materials to replace the conventional metallic structure materials, by hybrid structures, synthetic granite, Ferro-cement, fiber-reinforced concrete, and hydraulic cement concrete materials. It was reported that cementitious composite materials had good static and dynamic stability and might be an alternative material for the conventional material. J. Cho et al. [3] carried out a matrix of experiments on the epoxy matrix in carbon fiber/epoxy composite. The composite materials was modified with graphite nanoplatelets to improve their mechanical properties. Graphite nanoparticles were mixed and dispersed in the epoxy matrix by sonication, followed by a vacuum-assisted wet layup process. The composites reinforced with nanoparticles showed enhancement in compressive strength and in-plane shear properties. A simple analytical model was used to predict the longitudinal compressive strength, which was in good agreement with experimental results. However, specific structure materials that has high potential in machine element foundation application are still in early stage of investigations.

Epoxy granite (EG) composite materials EG became an alternative material to cast iron in machine base application [4–8]. Incorporation of granite particles into epoxy matrix demonstrated a remarkable reduction in stiffness with high damping and vibration characteristic [9] of the dynamic mechanical response of the fabricated EG composite beams. It was reported that the particle size and particles distribution of the filler material within epoxy matrix play a vital role in enhancing the mechanical and damping characteristics of structure composite materials. To enhance the toughness properties of EG composite structure materials, Kareem [10] incorporated polycarbonate (PC) into the EG. Although the EG/PC composite materials showed good mechanical properties, but the fabrication process is complicated and time consuming. Krishna et al. [11] demonstrated the performance of granite particles-reinforced epoxy composites fabricated at different weight concentration. Their results presented that the tensile and impact strength were increased by 2-fold granite powder-reinforced epoxy composite. Granite particles and fly ashes reinforced epoxy composites were fabricated by Ramakrishna and Rai [12] to investigate the effects of the two different fillers into the mechanical properties of EG materials. An attempt have also been made to use commercially available thermoplastic (polymethyl methacrylate) to improve the pure matrix device epoxy resin. The blend matrix was prepared at various polymethyl methacrylate and epoxy weight fractions. Then, a blended matrix with the highest strength was selected for composite preparation. Furthermore, Ramakrishna et. al [13] used unsaturated polyester as a matrix and granite powder reinforced with fly ash as fillers. The tensile and flexural strengths at various weight fractions of the fillers of these composites were assessed. The mechanical properties of granite powder composites were higher than fly ash composites. They modified this study [14] on granite-epoxy powder composites on toughening epoxy with unsaturated polyester and unsaturated polyester

with epoxy resin. Moreover, impact, compressive strength, and water absorption was investigated. It was concluded that a positive toughening effect was demonstrated by an improvement in the strength of the composites. On the other hand, the matrix of granite powder and fly ash was prepared by epoxy toughened with polymethylmethacrylate (PMMA) and various percent weights [15]. It was reported that the tensile and flexural strengths of the composite showed the highest value at 4% (w/w) of PMMA in the composites. The granite powder composites showed better properties than fly ash composites. Lately, they tried to use epoxy and acrylonitrile butadiene styrene (ABS)-toughened epoxy matrices as a matrix to granite powder [16]. Gonçalves et al. [17] studied the mechanical properties of a composite made of a mixture of epoxy resin and granitic stone powder. The mechanical properties included traction, flexion, compression, and hardness properties were presented. Chemical and mineralogical stone analyses and particle/matrix interface through SEM analyses were conducted. Venugopal et al. [18] numerically investigated the static and dynamic characteristic properties of epoxy granite columns with steel reinforcement. The proposed final configuration with standard steel sections had been modeled using finite element analysis for an equivalent static stiffness and natural frequencies of about 12–20% higher than the cast-iron structure. Therefore, the proposed finite element model of epoxy-granite-made vertical machining center column can be used as a viable alternative for the existing column to achieve higher structural damping. In spite of fracture toughness and mechanical properties of composite material were studied in several works [19–25] using various specimens' shapes such as compact tension or even center edge notch, the effects of granite particles size and particles shape have been never investigated.

It is speculated that different particles size of granite might induce synergistic effects on the mechanical, damping and fracture toughness properties of EG composite structure materials. The particle size of granite filler material did not be taken into consideration yet. Herien, for the first time, EG composite structure inexpensive materials were fabricated at different particle size and particles distribution of granite as a cost-effective materials to investigate these variations on mechanical properties and fracture toughness of the obtained EG materials. Accordingly, the focus of present study was to: (a) design a strong structure material for machine tool foundation application; (b) investigate the effect of granite particle size on mechanical properties (compressive strength, flexural strength and tensile modulus), the fracture toughness and the surface release energy or fracture strength of EG composite structure materials. The dynamic response of the proposed composite materials is not the scope of the present study and will be investigated in the future work.

2. Materials and methods

2.1. Materials

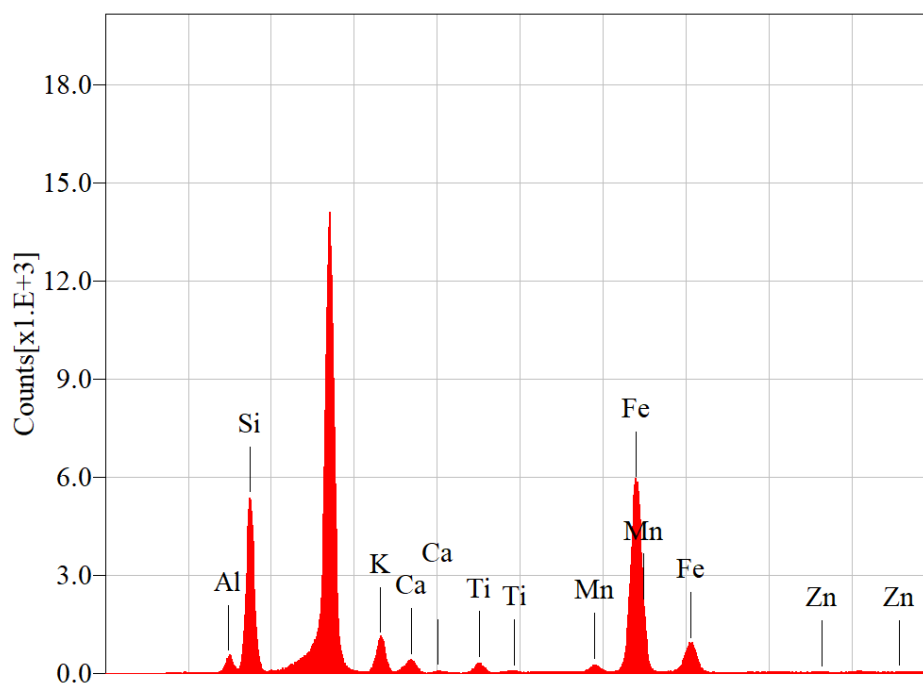
The specimen of epoxy granite is prepared by manual mixing of different sizes of granite particles which are crushed and sieved by a sieve analysis device with epoxy resin severally. The granite is founded in the south of Aswan in Shalateen in the far south of Egypt. X-ray fluorescence (XRF) analysis is performed for granite to know its chemical elements and the proportion of each element, this chemical analysis is shown in Table 1 and Figure 1. The epoxy resin is KEMAPOXY-150 RGL which is manufactured by Chemicals for Modern Buildings Company in Egypt (CMB). Kemapoxy 150 is a two components solvent-free, liquid epoxy compound, conforms to the standard specification ASTM C 881 [26], the epoxy mechanical properties are listed in Table 2.

Table 1. XRF chemical analysis of granite.

Element	ms%	mol%	Sigma
Al	8.5000	10.8068	3.7957
Si	47.6969	58.2576	4.1407
K	11.2912	9.9059	3.4859
Ca	3.5633	3.0498	2.9038
Ti	1.9455	1.3933	1.4508
Mn	1.1757	0.7342	1.0394
Fe	25.6899	15.7803	1.0007
Zn	0.1375	0.0722	1.2422

Table 2. Mechanical and physical properties of E-glass fiber and epoxy resin [27–29].

Properties	Kemapoxy (150 RGL)
Density (kg/m ³)	107 ± 2
Tensile strength (MPa)	50–100
Tensile modulus (GPa)	1.2–4.5
Passion ratio	0.35
In-plane shear modulus	1.24
Failure strain	1.7

**Figure 1.** XRF for granite particles.

2.2. Molding method

Plexiglass molds are 3 mm in thickness (Figure 2a), they are prepared for the composite specimen fabrication with dimensions which are shown in Figure 2b. Granite is crushed by a one-kilogram hammer then it is separated by a sieve analysis device into three different sizes divided as follows; coarse particles (C) that have a size range between 1.18–2.36 mm, medium particles (B) between 0.6–1.18 mm and fine particles (A) (powdered granite) less than 0.6 mm. The composite samples are fabricated in the mold at room temperature by varying granite particles size with a constant percentage of epoxy 12% by weight. The mixing ratio of the epoxy resin to hardener is 2:1. The different particle sizes of the granite were separately mixed with the epoxy in the mentioned proportions (12% epoxy, 88% granite particles) according to [30]. The mixture is poured into the molds (Figure 3) and subjected to hammering by light hammer and vibration to avoid the presence of gaps and voids between the particles and keep the size of the particle's constant. The specimens are kept in the molds for 24 h [30] then the specimens were taken out from the mold. And then left for 21 days to complete curing. Noting that all of this at normal conditions and room temperature. The sample densities and volume fraction are illustrated in Table 3. The weight fractions are measured using the ignition removal technique according to ASTM D3171-99 standard [31].

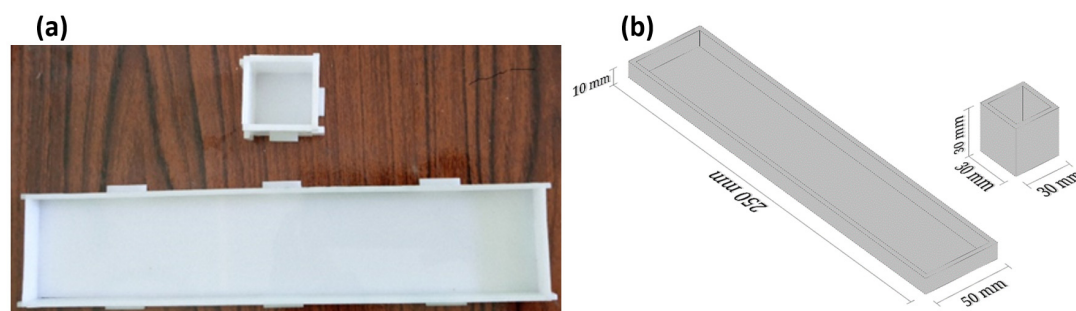


Figure 2. Mold of casting composite (a) plexiglass molds, (b) 3-D drawing with dimension.

Table 3. Epoxy granite specimen densities and weight fraction.

Specimen	Density (g/m^3)	Weight fraction granite (W_g) (%)	Weight fraction epoxy (W_e) (%)
Fine particles (A)	4.61	88.4	11.6
Medium particles (B)	4.43	87.5	12.4
Coarse particles (C)	4.21	85.3	14.6

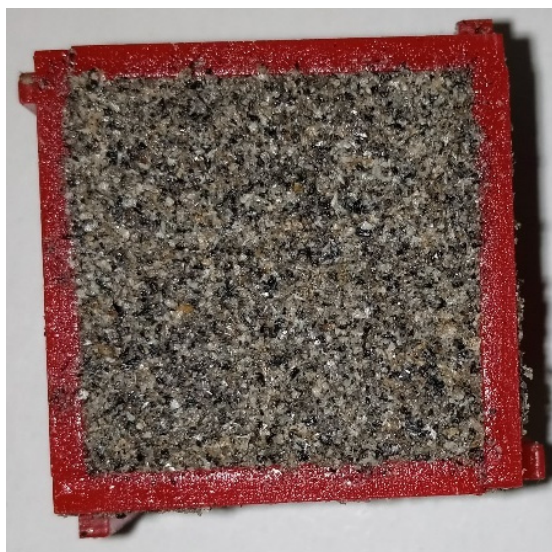


Figure 3. The specimens in the mold.

2.3. Mechanical properties

2.3.1. Compressive strength

A $30 \times 30 \times 30$ mm cubical test specimen is prepared for conducting compression tests. The compression test is carried out according to ASTM D2938-95 [32] using the computerized universal testing machine. Five specimens are prepared in each composition obtained by varying particles size in the mixture. The fabricated specimens photograph is shown in Figure 4. The compressive strength and flow curve are recorded and then plotted.

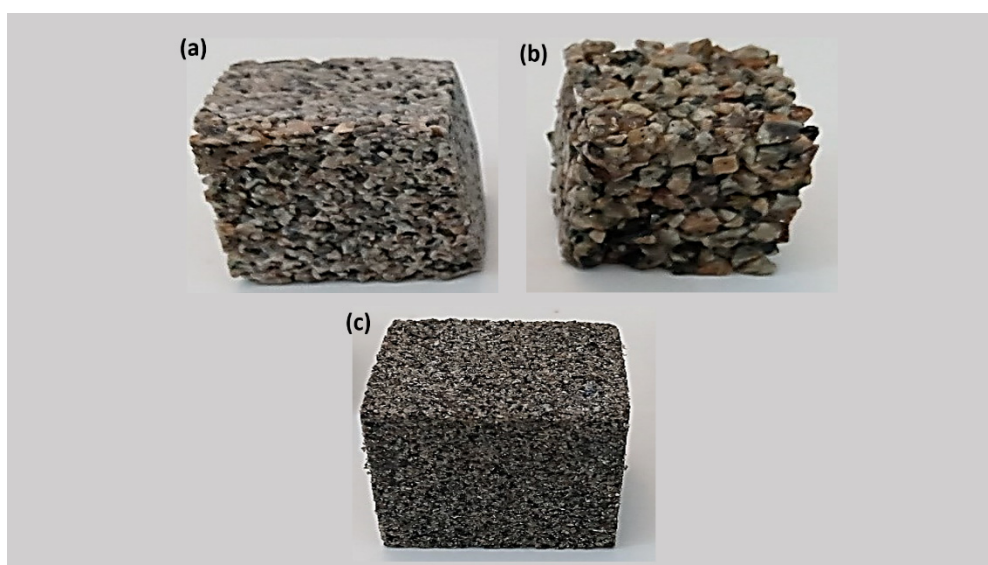


Figure 4. Compression test specimen: (a) fine particles, (b) medium, (c) coarse particles.

2.3.2. Flexure strength

The three points bending test is performed by using a universal test machine (Figure 5) and the specimens with dimensions of $250 \times 50 \times 10$ mm are fabricated (Figure 6) according to ASTM D790-03: standard [33]. The flexural strength and young modulus are calculated by the below Eqs 1 and 2.

$$\sigma = \frac{3F}{2bd^2} \quad (1)$$

$$E = \frac{l^3 F}{4bd^3 \delta} \quad (2)$$

where, F = load at a given point on the load-deflection curve (kN), l = support span (mm), b = width of test beam (mm), d = depth or thickness of tested beam (mm), and δ is maximum beam deflection.

This equation is valid in the case of elastic homogeneous materials, many works give the exact solution of this problem [34–36]. But this equation for simplicity and purposes of comparison of the three specimens with different particle size can be acceptable according to ASTM D790-03: Standard for unreinforced and reinforced plastics [33] and [37] and it can be acceptable for concert and other gravel reinforced material [38–40].

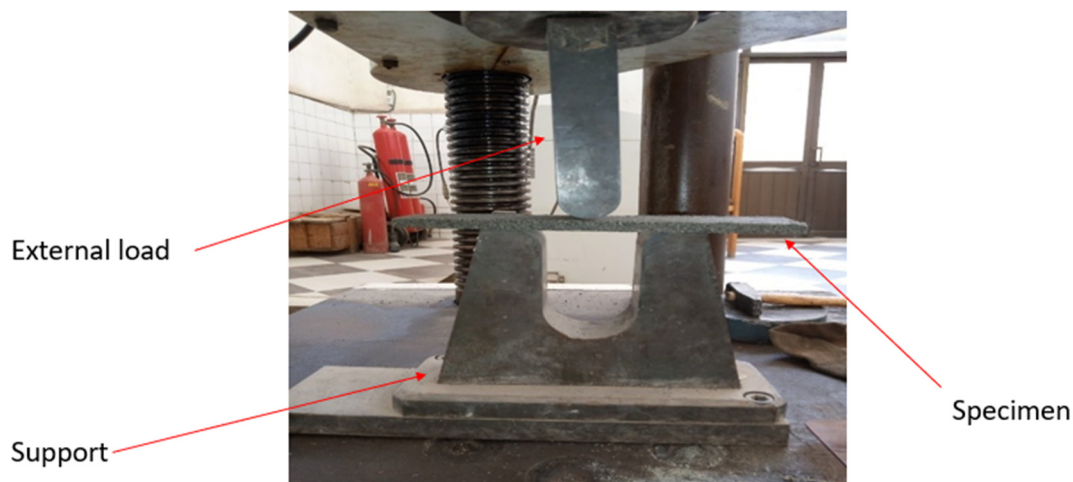


Figure 5. Three points bending test set up.



Figure 6. Flexural test specimens: (a) fine, (b) medium, (c) coarse particles.

2.3.3. Three-point single edge bending notch test

A single edge notch bending test (SENB) is carried out (Figure 7) to provide the values of fracture toughness. The specimens are fabricated (Figure 8) with length L of 200 mm, thickness w of 20 mm and width B of 15 mm to meet the following constraints span length = $4w$ and a notch length (a) such that $0.45 < a/B < 0.55$, these according to ASTM D5045-14: standard [41]. The reduction methods are as follow (Eqs 3 and 4) [42].

$$K_I = \frac{4F}{B} \sqrt{\frac{\pi}{w}} Y \quad (3)$$

$$Y = 1.63 \left(\frac{a}{w}\right)^{0.5} - 2.6 \left(\frac{a}{w}\right)^{1.5} + 12.3 \left(\frac{a}{w}\right)^{2.5} - 21.3 \left(\frac{a}{w}\right)^{3.5} + 21.9 \left(\frac{a}{w}\right)^{4.5} \quad (4)$$

where K_I is the fracture toughness, (a) pre-crack length w is plate thickness, Y is the geometric correction factor.

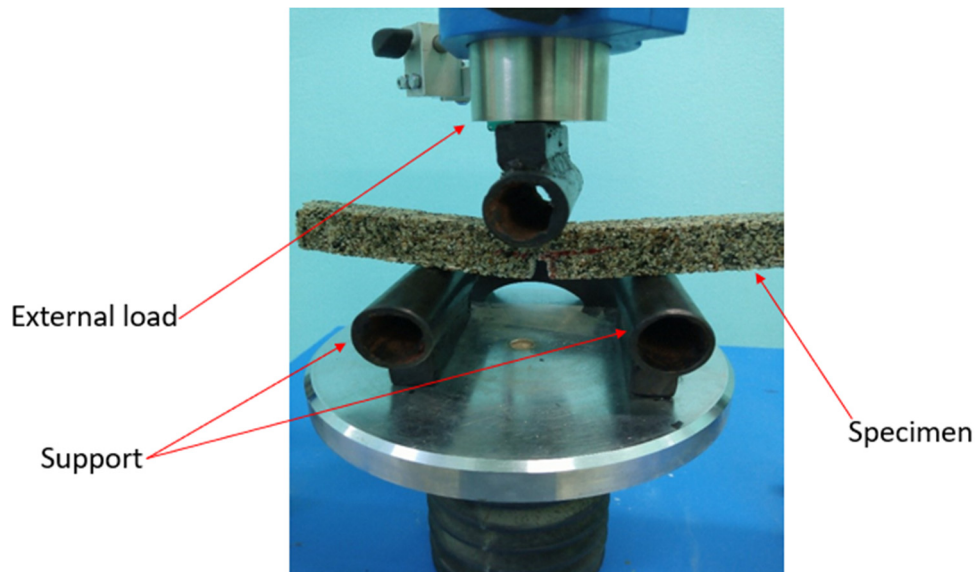


Figure 7. Single edge notch bending test.

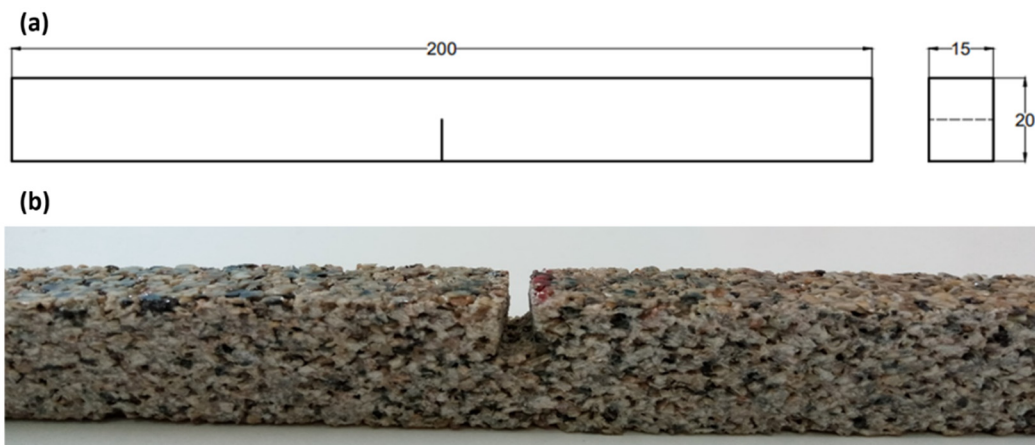


Figure 8. Test specimen of medium particles: (a) schematic drawing in mm (b) image.

3. Results and discussion

3.1. Compression test

Figure 9 shows the stress and strain curve of the compression test. It is measured that the compressive stress of composite specimen with fine particles (A), medium (B), and coarse (C) composite are (18.15, 13.785, and 10.444) MPa respectively. It is observed that the curve follows with the stress advanced is smooth not stepped especially with fine particles, this is an indication to the high consolidation and debonding of the material component. It is logical, that increasing of strength and young modulus of polymeric material for a specimen with fine particles reduced percentage elongation than that for medium and coarse particles as it is listed in Table 4; it is (0.13, 3.33, and 18.33) for fine, medium, and coarse particles respectively. The elastic modulus is relatively low compared to other monotonic material. The compressive strength of a specimen with fine

particulates than another specimen can be attributed to that compaction and debonding between particles increase with fine particles which means an increasing amount of granite than epoxy. This can be explained by the increasing density of specimens of fine particles than medium or coarse particles which are listed in Table 3. The failure modes are shown in Figure 10, the severe cracking and breaking are observed in all specimen while the cracks in a specimen with coarse particle (Figure 10c) is little, this because the large particles resist the crack propagates. The Fracture mode in a specimen with fine particles (Figure 10a) damage occurs in the whole body of the specimen, this is due to the lower bridging takes places in the direction of loading at the crack faces ahead of crack initiation, this tends to make brittleness of the specimen increase. Hence, the area of the specimen (A) less than in specimen B or C. SEM analysis is illustrated in Figure 11, it is observed that in specimen (A) the amount of epoxy is very little (11.6%) as it is not observed in the image (Figure 11a), but it just bonds the particles each other, therefore, the load just carried by granite, at this time the strength increase while lack of debonding between particles increases brittleness increase and reduced the ductility as the material cannot withstand the load for long times. The epoxy resin in the specimen (B) has a larger amount (Figure 11b) therefore it an intersection between particles, therefore, it takes part of the total load, hence the strength decreases while ductility is increased, it is also observed granite particles/epoxy debonding mode and granite pull out from the matrix. Figure 11c illustrate the reason for decreasing strength while ductility increase, this due to that larger size granite particles adhered with a larger amount of resin at a small area, therefore the granite easy can leave the resin in the matrix, therefore ductility is increased and softening.

Table 4. Compression test results.

Element	Compressive strength (MPa)	Elastic modulus (MPa)	Percentage increase in surface area (%)	Reduction in length (%)
Fine particles (A)	18.15	1200	0.070	0.13
Medium particles (B)	13.75	572	6.47	3.33
Coarse particles (C)	10.44	531.09	41.66	18.33

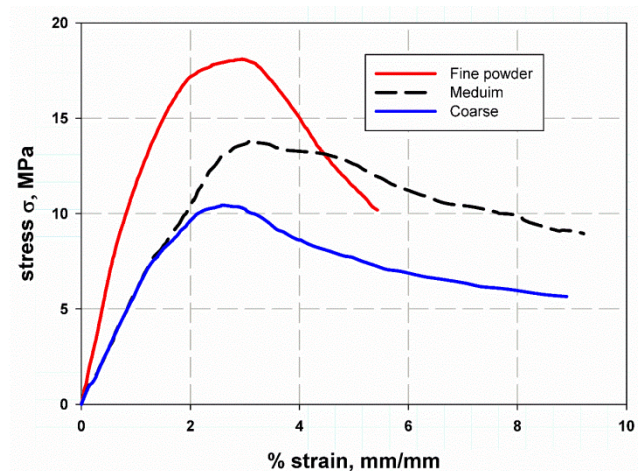


Figure 9. Stress and strain curve for compression test.

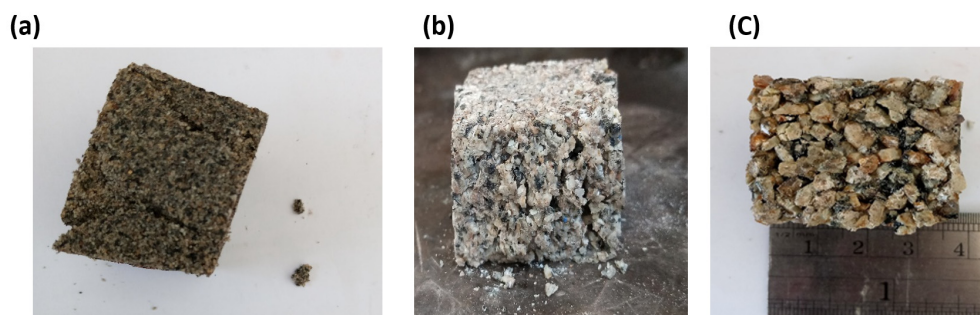


Figure 10. Modes of failure under compression (a) fine, (b) medium, (c) coarse.

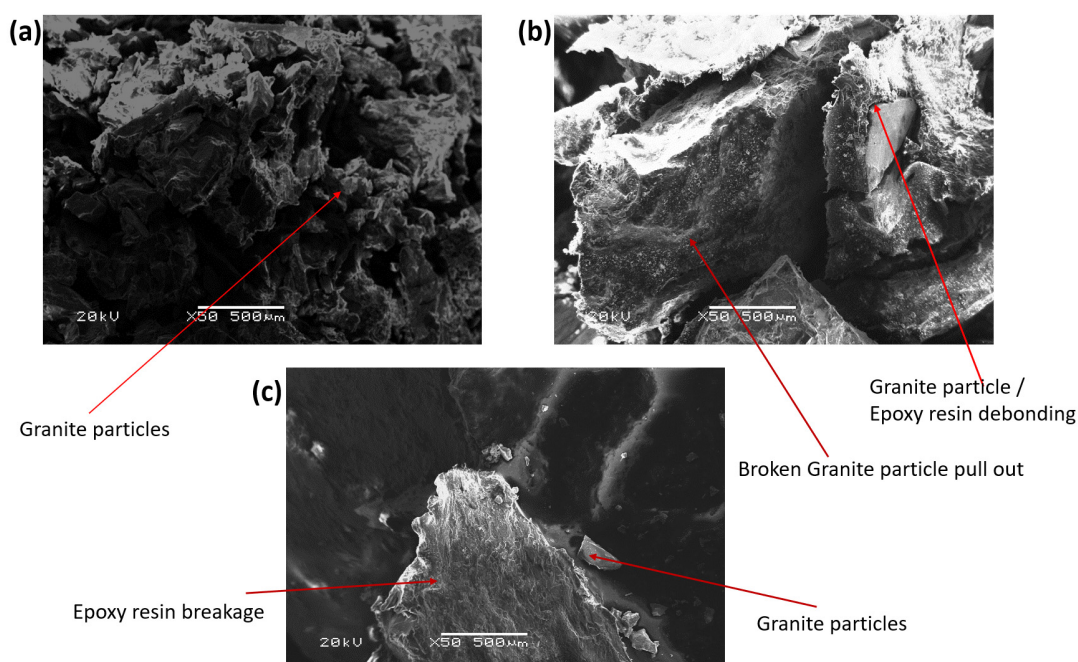


Figure 11. SEM image for (a) fine particles, (b) medium, (c) coarse.

3.2. Flexural

Figure 12 shows flexural stress and deflection strain curve, it is observed that specimen (A) with fine particles has the greatest strength value than specimen (B) with medium particles or (C) with coarse size particles (Table 5). The curve flow is not smooth as the damage fast collapses, this can be attributed to that debonding between particles and epoxy is not strong and the number of granite particles that resist crack is little. It is well observed through the brittle fracture modes illustrated in Figure 13. Focus, observation for a specimen with coarse particles, it is seen a large steep between data, this is due to granite particles pull out from the matrix. The flexural modulus is maximum for coarse particles (9.588 MPa), with a lower strength (11.25 MPa) and ductility, this means weak bonding with the epoxy resin. The curves nearly have the same trend; get maximum suddenly, then suddenly decrease. This is due to granite particles suddenly resist the load as the granite leaves the matrix, hence the failure takes place. The flexural modulus of specimens (B) has lower values, due to

the amount of voids inside the specimen is larger than others, and also the average thickness is larger than other specimens therefore, the I moment of area is larger.

Table 5. Flexural strength and modulus.

Element	Flexural strength (MPa)	Flexural modulus (GPa)
Fine particles (A)	20.137	5.285
Medium particles (B)	16.36	2.600
Coarse particles (C)	11.25	9.588

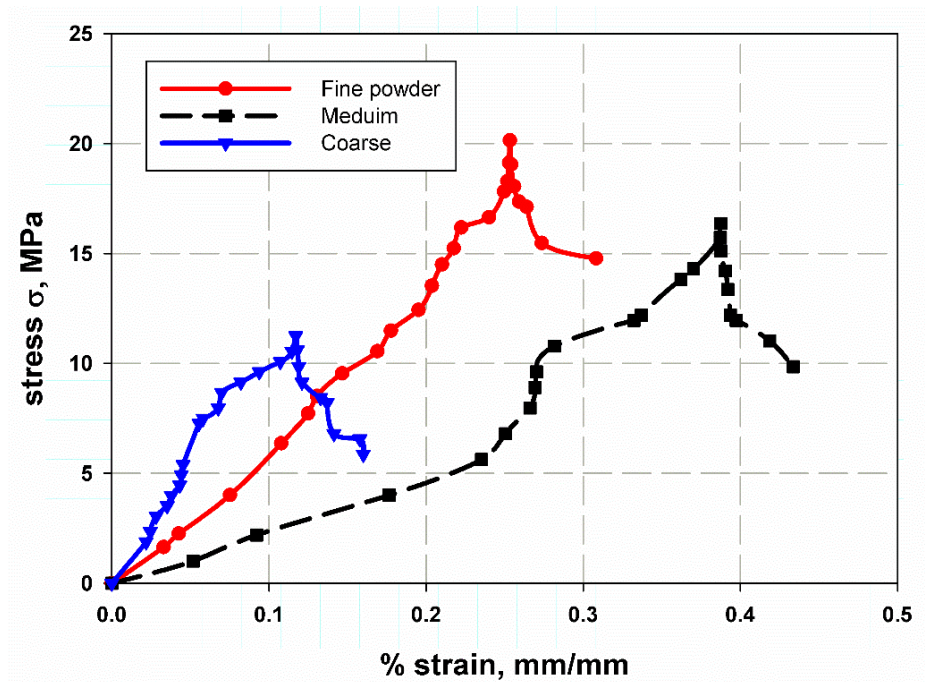


Figure 12. stress and strain curve for the flexural test.

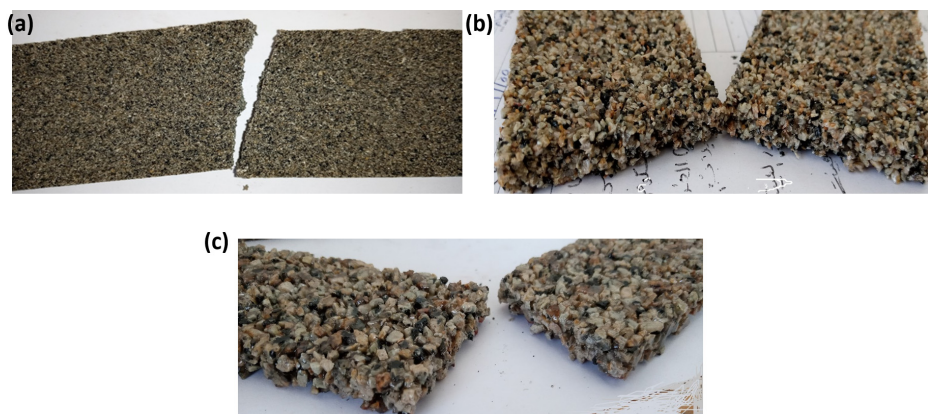


Figure 13. Modes of failure under bending load for particles of (a) fine size, (b) medium size, (c) coarse size.

3.3. Three-point single edge notch bending (SENB)

To measure fracture toughness of cracked specimen of such material, the SENB standard specimen is used. The curve of load and deflection is plotted in Figure 14, the maximum values of bending load are 156, 151 and 72 N for specimen (A), specimen (B) and specimen (C) respectively. These loads implemented in Eq 3, then the fracture toughness K_{IC} is measured as (24.73, 23.94 and 11.41 $Pa\sqrt{m}$) for specimen (A), specimen (B), and specimen (C) respectively (Table 6). The values of fracture toughness for specimens A and B are closely and relatively high than that with larger size specimens (C). This is due to the increasing weight fraction of granite (Table 3) which resists crack propagation, it also makes bridging the two faces of cracks. The fracture modes are purely mode I, therefore, the direction of crack through the loading action (Figure 15).

Table 6. Values of fracture toughness for specimens.

Specimen	Maximum force (N)	Average fracture toughness ($MPa\sqrt{m}$)
Fine particles (A)	156	24.73
Medium particles (B)	151	23.94
Coarse particles (C)	72	11.41

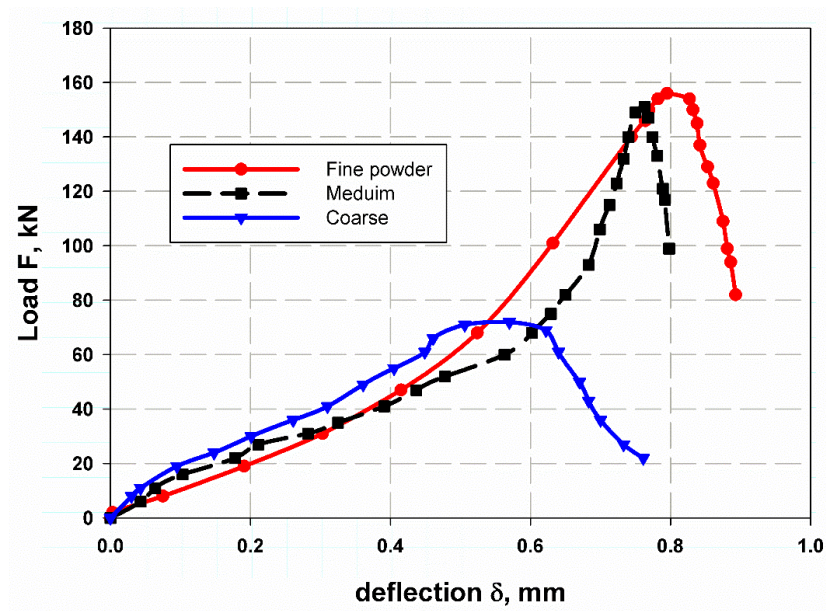


Figure 14. Force and deflection curve of SENB.

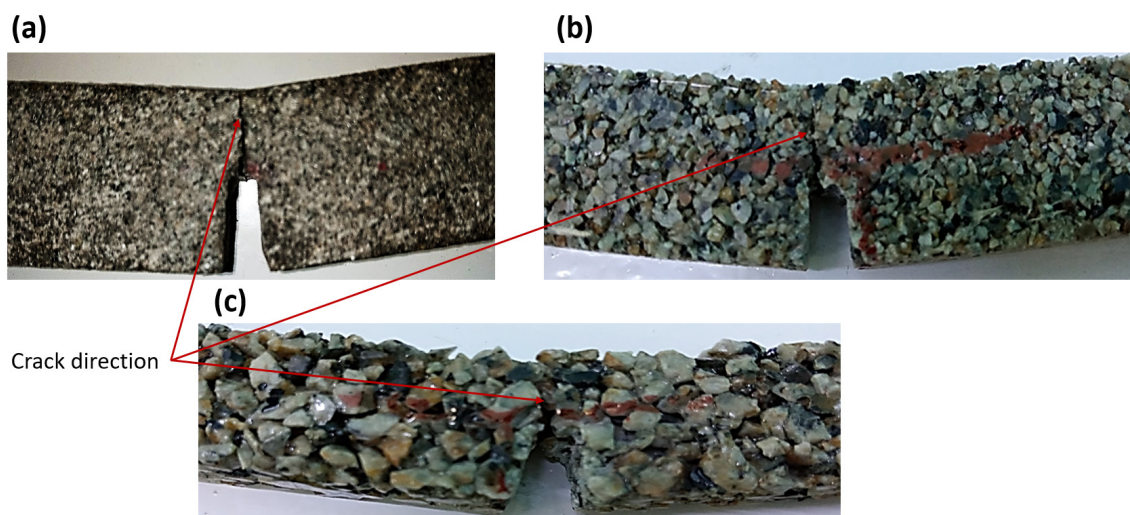


Figure 15. Modes of failure under three-point single edge notch bending of particle size (a) fine, (b) medium, (c) coarse.

4. Conclusions

We have successfully fabricated epoxy granite composite structure materials at three different of the granite particles size. The effects of the coarse, medium and fine granite particles on the mechanical properties, such as compressive strength and flexure strength were investigated. Furthermore, the fracture toughness, single edge notch bending test and damping capacity of the fabricated EG composite materials were also assessed. Interestingly, the results showed that the compressive strength of the EG composite induced the highest value at fine particles size. The values of compressive strength were 18.15, 13.75 and 10.44 MPa. whereas, the average fracture toughness's were 24.73, 23.94 and 11.91 $MPa\sqrt{m}$ for fine (≤ 0.6 mm), medium (0.6–1.18 mm), and coarse (1.18–2.36 mm) granite particles, respectively. In addition, the average flexural strengths and flexural young's modulus showed a 20.13 MPa and 5.28 GPa for fine and 11.25 MPa and 9.58 GPa for coarse granite particles, respectively. It can be concluded that fabrication of EG composite structure materials with fine granite particles (≤ 0.6 mm) with a dequite mechanical properties and good durability might have be a potential candidate as a new machine element foundation tools.

Conflict of interest

All authors declare no conflicts of interest in this paper.

References

1. Rahman M, Mansur A, Karim B (2001) Non-conventional materials for machine tool structures. *JSME Int J C-Mech Sy* 44: 1–11.
2. Gorninski JP, Dal Molin DC, Kazmierczak CS (2004) Study of the modulus of elasticity of polymer concrete compounds and comparative assessment of polymer concrete and portland cement concrete. *Cem Concr Res* 34: 2091–2095.

3. Cho J, Chen JY, Daniel IM (2007) Mechanical enhancement of carbon fiber/epoxy composites by graphite nanoplatelet reinforcement. *Scripta Mater* 56: 685–688.
4. Do Suh J, Kim HS, Kim JM (2004) Design and manufacture of composite high speed machine tool structures. *Compos Sci Technol* 64: 1523–1530.
5. Suh JD, Lee DG (2008) Design and manufacture of hybrid polymer concrete bed for high-speed CNC milling machine. *Int J Mech Mater Des* 4: 113–121.
6. Kim HS, Park KY (1995) A study on the epoxy resin concrete for the ultra-precision machine tool bed. *J Mater Process Tech* 48: 649–655.
7. Orak S (2000) Investigation of vibration damping on polymer concrete with polyester resin. *Cement Concrete Res* 30: 171–174.
8. Piratelli-Filho A, Levy-Neto F (2010) Behavior of granite-epoxy composite beams subjected to mechanical vibrations. *Mater Res* 13: 497–503.
9. Selvakumar A, Mohanram PV (2012) Analysis of alternative composite material for high speed precision machine tool structures. *Ann Fac Eng Hunedoara* 10: 95.
10. Kareem AA (2013) Mechanical properties of granite powder as a filler for polycarbonate toughened epoxy resin. *Int J Pharm Sci Res* 3: 254–257.
11. Krishna HVR, Priya SP, Rai SK, et al. (2005) Tensile, impact, and chemical resistance properties of granite powder-epoxy composites. *J Reinf Plast Comp* 24: 451–455.
12. Ramakrishna HV, Rai SK (2005) A Study on the mechanical and water absorption properties of granite powder/epoxy toughened with PMMA and fly ash/epoxy toughened with PMMA composites. *J Reinf Plast Comp* 24: 1809–1816.
13. Ramakrishna HV, Priya SP, Rai SK, et al. (2005) Tensile, flexural properties of unsaturated polyester/granite powder and unsaturated polyester/fly ash composites. *J Reinf Plast Comp* 24: 1279–1287.
14. Ramakrishna HV, Rai SK (2006) Effect on the mechanical properties and water absorption of granite powder composites on toughening epoxy with unsaturated polyester and unsaturated polyester with epoxy resin. *J Reinf Plast Comp* 25: 17–32.
15. Ramakrishna HV, Priya SP, Rai SK, et al. (2005) Studies on tensile and flexural properties of epoxy toughened with PMMA/granite powder and epoxy toughened with PMMA/fly ash composites. *J Reinf Plast Comp* 24: 1269–1277.
16. Ramakrishna HV, Priya SP, Rai SK (2007) Flexural, compression, chemical resistance, and morphology studies on granite powder-filled epoxy and acrylonitrile butadiene styrene-toughened epoxy matrices. *J Appl Polym Sci* 104: 171–177.
17. Gonçalves JAV, Campos DAT, Oliveira GJ, et al. (2014) Mechanical properties of epoxy resin based on granite stone powder from the Sergipe fold-and-thrust belt composites. *Mater Res* 17: 878–887.
18. Venugopal PR, Kalayarasan M, Thyla PR, et al. (2019) Structural investigation of steel-reinforced epoxy granite machine tool column by finite element analysis. *P I Mech Eng L-J Mat* 233: 2267–2279.
19. Abdellah MY (2017) Essential work of fracture assessment for thin aluminium strips using finite element analysis. *Eng Fract Mech* 179: 190–202.
20. Abdellah MY, Fathi HI, Abdelhaleem AMM, et al. (2018) Mechanical properties and wear behavior of a novel composite of acrylonitrile–butadiene–styrene strengthened by short basalt fiber. *J Compos Sci* 2: 34.

21. Fouad H, Mourad AHI, ALshammari BA, et al. (2020) Fracture toughness, vibration modal analysis and viscoelastic behavior of Kevlar, glass, and carbon fiber/epoxy composites for dental-post applications. *J Mech Behav Biomed Mater* 101: 103456.
22. Hassan MK, Abdellah MY, Azabi SK, et al. (2015) Fracture toughness of a novel GLARE composite material. *IJET-IJENS* 15: 36–41.
23. Mohammed Y, Hassan MK, Hashem AM (2014) Effect of stacking sequence and geometric scaling on the brittleness number of glass fiber composite laminate with stress raiser. *Sci Eng Compos Mater* 21: 281–288.
24. Vipulanandan C, Dharmarajan N (1998) Effect of temperature on the fracture properties of epoxy polymer concrete. *Cement Concrete Res* 18: 265–276.
25. Gomes MLPM, Carvalho EAS, Demartini TJC, et al. (2020) Mechanical and physical investigation of an artificial stone produced with granite residue and epoxy resin. *J Compos Mater*.
26. Garner NC (2019) Epoxy Bonding Adhesive: ASTM C 881. Available from: <http://summitgc.net/wp-content/uploads/2019/08/Garner-Project-Specifications.pdf>.
27. Jones RM (1998) *Mechanics of Composite Materials*, 2Eds., Boca Raton: CRC Press.
28. Mallick PK (1997) *Composites Engineering Handbook*, 1 Ed., Boca Raton: CRC Press.
29. Lu N, Swan Jr RH, Ferguson I (2012) Composition, structure, and mechanical properties of hemp fiber reinforced composite with recycled high-density polyethylene matrix. *J Compos Mater* 46: 1915–1924.
30. McKeown PA, Morgan GH (1979) Epoxy granite: a structural material for precision machines. *Precis Eng* 1: 227–229.
31. ASTM D3171-99. Standard test methods for constituent content of composite materials. ASTM International, 1999. Available from: <https://www.astm.org/DATABASE.CART/HISTORICAL/D3171-99.htm>.
32. ASTM D2938-95. Standard test method for unconfined compressive strength of intact rock core specimens. ASTM International, 2002. Available from: <https://www.astm.org/Standards/D2938>.
33. ASTM D790-07. Standard test methods for flexural properties of unreinforced and reinforced plastics and electrical insulating materials. ASTM International, 2007. Available from: <https://www.astm.org/DATABASE.CART/HISTORICAL/D790-07.htm>.
34. Chen Y, Han X, Hu X, et al. (2020) Statistics-assisted fracture modelling of small un-notched and large notched sandstone specimens with specimen-size/grain-size ratio from 30 to 900. *Eng Fract Mech* 235: 107134.
35. Han X, Chen Y, Hu X, et al. (2019) Granite strength and toughness from small notched three-point-bend specimens of geometry dissimilarity. *Eng Fract Mech* 216: 106482.
36. Ahmed M, Mallick J, Hasan MA (2016) A study of factors affecting the flexural tensile strength of concrete. *J King Saud Univ Eng Sci* 28: 147–156.
37. Zweben C, Smith WS, Wardle MW (1979) Test methods for fiber tensile strength, composite flexural modulus, and properties of fabric-reinforced laminates, *Composite Materials: Testing and Design (Fifth Conference)*, 228–262.
38. Harish BA, Hanumesh BM, Siddesh TM, et al. (2016) An experimental investigation on partial replacement of cement by glass powder in concrete. *Int Res J Eng Tech* 3: 1218–1224.
39. Denton NL, Magill MA, Hillsman VS, et al. (2000) *Strength of Materials Laboratory Manual*, West Lafayette: Learning Systems Incorporated.

40. Ajamu SO, Ige JA (2015) Effect of coarse aggregate size on the compressive strength and the flexural strength of concrete beam. *Int J Eng Res Appl* 5: 67–75.
41. ASTM D5045-99, Standard test methods for plane-strain fracture toughness and strain energy release rate of plastic materials. ASTM International, 1999. Available from: <https://www.astm.org/DATABASE.CART/HISTORICAL/D5045-99.htm>.
42. Bower AF (2009) *Applied Mechanics of Solids*, 1 Ed., Boca Raton: CRC Press.



AIMS Press

© 2021 the Author(s), licensee AIMS Press. This is an open access article distributed under the terms of the Creative Commons Attribution License (<http://creativecommons.org/licenses/by/4.0>)